JOURNAL OF MATERIALS SCIENCE 25 (1990) 3203–3207

Effect of fluoride, chloride and carbonate ions introduced by cyclic pH fluctuation on the physico-chemical properties of apatite-based ceramics

A. KRAJEWSKI, A. RAVAGLIOLI
Istituto di Ricerche Tecnologiche per la Ceramica del CNR, via Granarolo 64, 48018 Faenza (Ravenna), Italy

N. ROVERI
Centro di Studio per la Fisica delle Macromolecole del CNR, c/o Dipartimento di Chimica "G. Ciamician", via Selmi 2, 40126 Bologna, Italy

A. BIGI, E. FORESTI
Dipartimento di Chimica "G. Ciamician", via Selmi 2, 40126 Bologna, Italy

A structural, chemical and thermal investigation has been carried out on apatites submitted to cyclic pH fluctuation in the presence of fluoride, chloride and carbonate ions. Unlike fluoride, chloride is not appreciably incorporated into the apatite structure under cyclic pH fluctuation. However, the presence in solution of one of these ions inhibits carbonate substitution for phosphate groups in the apatite structure. The results reveal that grain growth during sintering is similar for the different samples, while slight differences in some technological properties (contraction during firing, softening point, etc) of sintered apatites have been detected.

1. Introduction

Hydroxyapatite (HA), whose chemical formula is $Ca_{10}(PO_4)_6(OH)_2$, represents the most widely investigated crystalline biomaterial [1], due to the fact that its composition is very close to that of the mineral component of bone and tooth. Biological apatites are known for their occurrence in non-stoichiometric form, usually with low values of the Ca/P ratio, and exhibit structural imperfections such as defects and atomic substitution with substantial amounts of foreign ions such as CO_3^{2-}, F^-, Cl^-, Mg^{2+}, Na^+, K^+ and other cations [2, 3]. Carbonate groups can partially substitute for OH^- (site A) and/or PO_4^{3-} (site B) groups in the crystal lattice of synthetic apatites [4, 5], while fluoride and chloride ions can substitute for the OH^- group in a whole range of compositions [6]. Synthetic carbonate apatites usually display reduced crystallinity, wheras biological apatites appear to become more crystalline as the carbonate content increases.

Studies on the extent of dissolution in acids of apatites containing both fluoride and carbonate ions have shown that the contribution of F^- in promoting a regular arrangement of the molecular packing into the crystal lattice, a factor that fosters the crystalline state stability of the apatite, is more significant than the opposite randomizing effect due to the presence of carbonate groups [7]. Furthermore, a study carried out on the interaction of fluoride and carbonate ions dissolved in the mother liquor with the hydroxyapatite structure, under conditions of cyclic pH fluctuation, showed that carbonate incorporation into the apatite structure seems to be hindered by the contemporary presence of fluoride [8]. The crystallographic A site of the apatite unit cell is filled in an obvious best way by monoatomic anions (such as F^-, Cl^-), whereas polyatomic anionic groups (such as CO_3^{2-}, OH^-, etc.) require a slight rearrangement of the positions of the neighbouring atoms for steric reasons. The OH^- group fills the A sites with the O–H bond direction parallel to the c axis [9]. The A site coincides with the geometrical centre of the Ca^{2+} triangles lying on the mirror planes at $z=1/4$ and $z=3/4$ of the crystallographic unit cell. The oxygen atoms of the O–H groups lie either above or below these planes by about 0.03 nm (on the average) and the O–H direction always points away from the mirror plane.

The highest structural order is that in which rows of aligned sequential O–H groups are equiversed (–OH . . .–OH . . . –OH . . .) in one direction as shown in Fig. 1a. This ideal arrangement gives rise to a local high dipolar moment which derives from the vectorial sum of the dipolar moment of each contributing O–H group. The dipolar interactions among the rows contribute to destabilize such an ordered arrangement. The OH^- randomly organized arrangement like that outlined in Fig. 1b is then the most probable, with 50% of the O–H groups directed in one way and the other 50% in the opposite way. This arrangement confers a certain degree of disorder on

0022–2461/90 $03.00 + .12

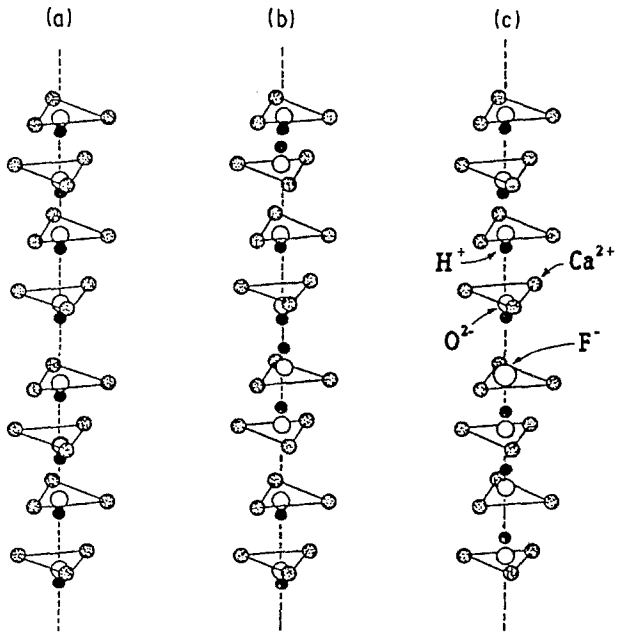

Figure 1 Picture of different possible arrangements of the O–H group: (a) infinite equiversed model; (b) random model (note the O–H H–O short distance at the versus change points); (c) long stacks of equiversed O–H groups induced by the polarizing presence of a fluorine atom in the A site.

the apatite structure of hydroxyapatite. If two adjacent O–H groups point towards each other from the mirror planes at $z=1/4$ and $z=3/4$, there would be steric interference between them. Thus a reversal of the O–H direction requires that an intermediate A site is vacant or filled with a halogen atom. If one F^- ion is placed in an A site, then it would exert at least a slight attraction for the hydrogen atoms of the two neighbouring OH groups, inducing a preferential orientation of the groups as shown in Fig. 1c. Therefore, along a row of O–H groups the sequence is often interrupted and the direction of equiversed O–H groups is reversed after every interruption.

The length of each interval depends obviously on the particular chemico-physical condition that occurred at the crystallization time. Long intervals of equiversed O–H groups can be obtained only by operating with very long times of crystallization, at a temperature as low as possible, near to the thermodynamic equilibrium conditions (very difficult to achieve), or by the action of enzymatic catalysts (possible in living bones of vertebrate animals). However, up-to-date technological know-how about this kind of bioengineering process is completely lacking. However, another possibility exists: since F^- is more tightly bound to the structure than OH^-, in partially fluoride-substituted HA the hydroxyl ions hydrogen-bonded to F^- are more tightly bound than those not so hydrogen-bonded, because of the higher polarizability of the fluoride with respect to the oxygen. Thus a very small amount of fluoride-substituted hydroxyl ions in the A site drives the building of quite long rows of equiversed O–H groups. This gives rise to a fairly well ordered apatitic structure, and it is sufficient to imbue hydroxyapatite with a large part of the thermodynamic properties of fluoroapatite [6]. Also in chloride-substituted apatites an interaction based on hydrogen bonding takes place between chloride and hydroxyl ions. However, since the electronegativity and the binding energy in the structure are less for Cl^- than for OH^-, the hydrogen bonding between Cl^- and OH^- does not necessarily increase the stability of the structure.

In order to investigate the effect of the interaction of fluoride, chloride and carbonate with HA on the physical-chemical properties of apatite-based ceramics, a structural, chemical, thermal and electron microscope investigation has been carried out on apatites submitted to cyclic pH fluctuation in the presence of fluoride, chloride and carbonate.

2. Experimental procedure

2.1. Materials

Hydroxyapatite was prepared by the neutralization of a continuously stirred $Ca(OH)_2$ aqueous suspension with H_3PO_4 at 100° C. The product was filtered, washed with distilled water and dried at 100° C.

The incorporation of fluoride and chloride into the apatite structure was carried out in an aqueous medium employing the cyclic pH variation technique described by Duff [10] for the synthesis of fluoroapatite. 10 g of hydroxyapatite was placed in a polythene bottle with 500 ml of a 0.01 M aqueous solution of sodium fluoride or chloride. This system was equilibrated at pH 7 overnight, then the pH was dropped to 4 with 1 M HNO_3. After 30 min of equilibration, the pH was raised to 7 using 1 M NaOH. This cycle of pH fluctuation was repeated three times and the solid phase was filtered, washed with distilled water and dried at 100° C. A further series of products was prepared using pH 13 as the upper limit.

2.2 Methods

X-ray diffraction was carried out using a Philips powder diffractometer using nickel-filtered Cu$K\alpha$ radiation. The 2θ range covered was from 10 to 65° at a scanning speed of 0.5° min^{-1}. The lattice constants were determined from diffractometric data using least-squares refinement.

For infrared (IR) absorption analysis, 1 mg of the powdered samples was carefully mixed with 300 mg of KBr (infrared grade) and pelletized under vacuum. The pellets were analysed using a Perkin-Elmer 380 IR grating spectrophotometer, range 4000 to 400 cm^{-1}, with a normal slit and scanning speed of 50 min.

The fluoride content (expressed as fluoride at %, where 100 at % corresponds to the total substitution of F^- for OH^-) was determined using the potentiometric method reported by Duff and Stuart [11] using an HCl–trisodium citrate buffer, pH 5.4. The

TABLE I Lattice constants of the apatitic products obtained after HA interaction with Cl^- (0.01 M) and F^- (0.01 M) under cyclic pH fluctuation

Sample	pH range	X^- (at %)	a (nm)	c (nm)
F1	4 to 7	21.0	0.9399(4)	0.6883(4)
F2	4 to 13	22.0	0.9399(4)	0.6884(4)
Cl1	4 to 7	–	0.9416(5)	0.6881(5)
Cl2	4 to 13	–	0.9415(6)	0.6881(5)

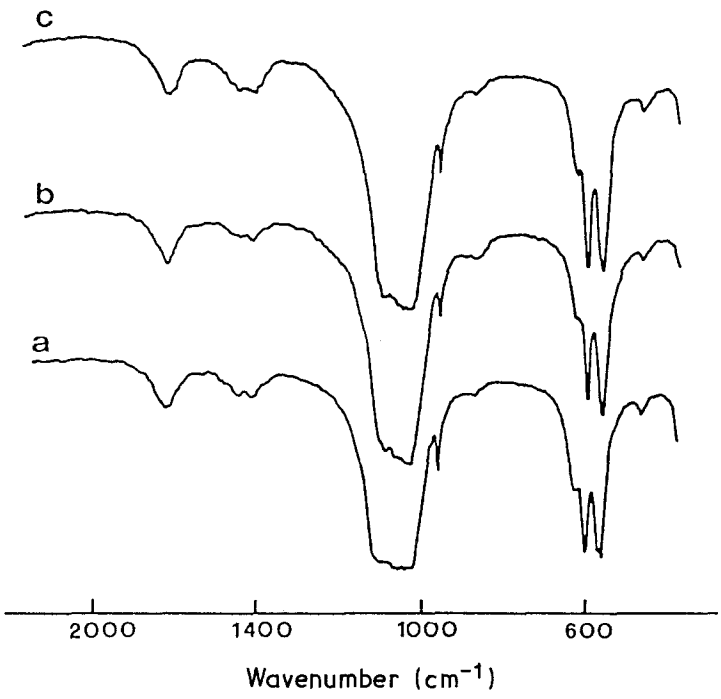

Figure 2 Infrared absorption spectra of (a) HA, (b) C11 and (c) C12.

detecting system was a Radiometer type PY-ZF1052F fluoride-sensitive electrode and a Radiometer type K 401 reference electrode fitted to an Amel type 337 pH meter. Chloride content was determined by a differential electrolytic potentiometric method according to Bishop and Dhaneshwar [12].

Compaction was carried out in a die measuring 5 × 11 cm using a pressure of 300 kg cm^{-2}. The tablets thus obtained were fired at different temperatures from 900 to 1300° C in a preheated kiln. Firing was carried out for 1, 8, 12 and 48 h.

A Leitz Wetzlar microscope type 307-107.003 514637 equipped with a heating plate (in a small horizontal tubular furnace) and a photographic camera was used to determine the shrinkage of cubic-shaped samples (1 mm x 1 mm x 1 mm) sintered at 1000° C. Scanning electron microscopy was carried out using a Philips SEM 501; specimens were mounted using colloidal silver and coated in vacuum with gold.

Differential thermal analysis (DTA) and differential thermogravimetry (DTG) were performed either with air convective flow or with conductive heating alone to assess the different behaviour in air or in a closed system. Model 404/2 and model 429/316 Netzch Kilns apparatuses were used. The rate of heating was 5° C min^{-1} up to 1200° C.

3. Results

The lattice constants calculated for HA are a= 0.9435(3) nm, c=0.6884(2) nm. The X-ray diffraction patterns of the solid products obtained after HA interaction with fluoride in the range of pH 4 to 7 (Fl) and 4 to 13 (F2) and with chloride in the range of pH 4 to 7 (C11) and 4 to 13 (C12) show the diffraction maxima characteristic of a crystalline apatitic phase. The lattice parameters calculated for the different products are reported in Table I together with their fluoride and chloride content. The IR spectra of the different apatitic products show the characteristic absorption bands of PO_4^{3-} and OH^- groups, together with the bands at 1455 to 1430 and 870 cm^{-1} characteristic of carbonate. Fig. 2 shows the infrared absorption spectra of HA (Fig. 2a) and HA after interaction with chloride in the range of pH 4 to 7 (Fig. 2b) and 4 to 13 (Fig. 4c). The infrared spectra of HA after interaction with fluoride are very close to those obtained after interaction with chloride in the same range of pH.

The weight losses of the apatitic products submitted

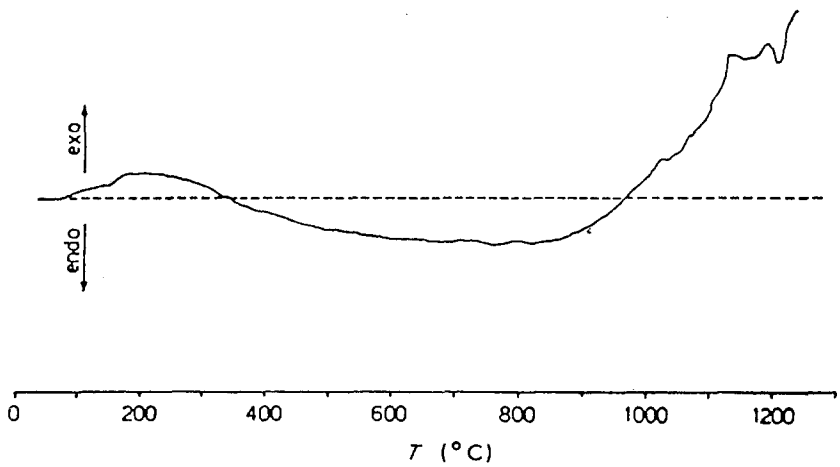

Figure 3 DTA curve of C11: mass 0.1 g, sensitivity 0.1 mV, dT/dt = 5.0° C min^{-1}.

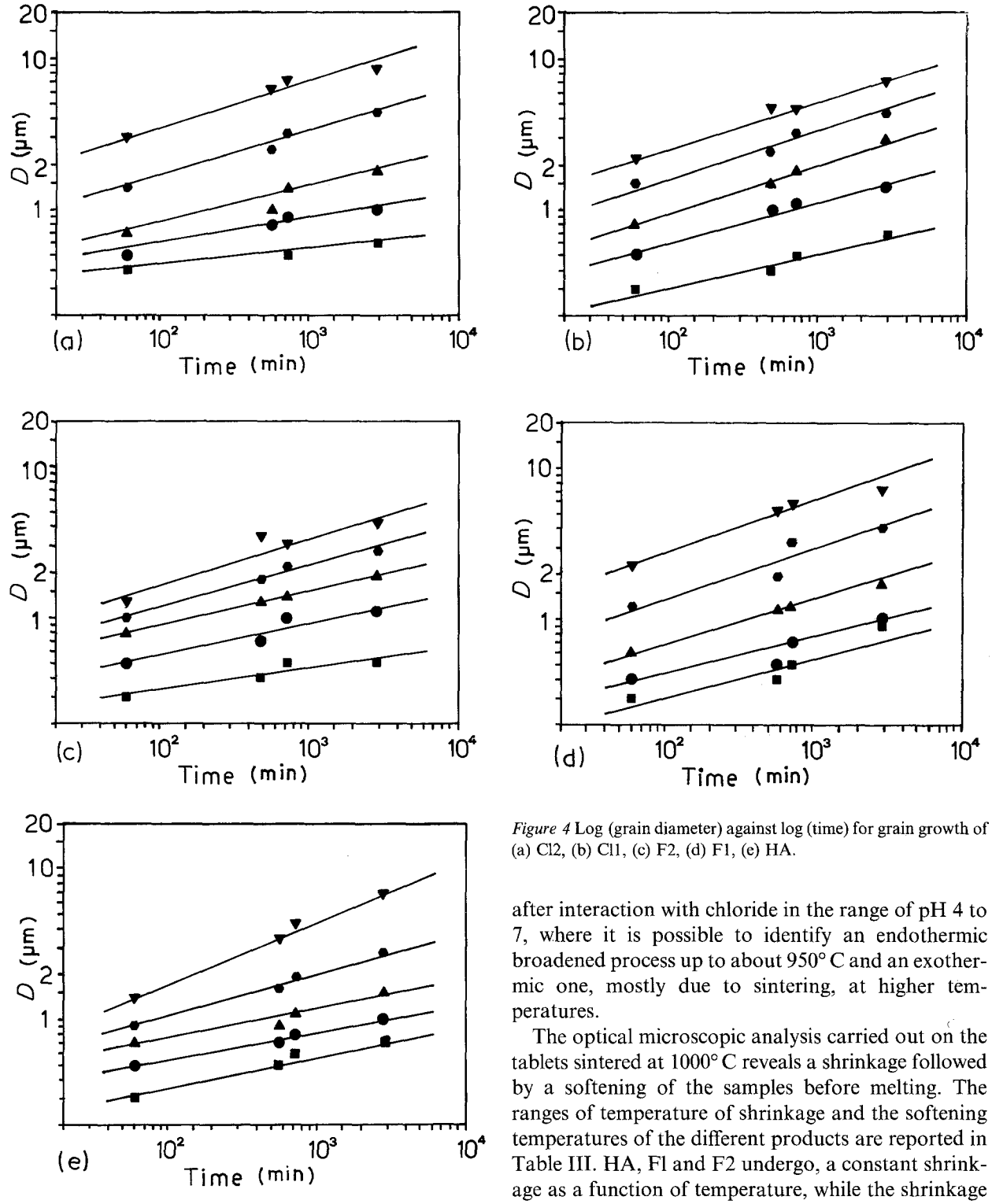

Figure 4 Log (grain diameter) against log (time) for grain growth of (a) C12, (b) C11, (c) F2, (d) F1, (e) HA.

to thermogravimetric analysis are reported in Table II. The differential thermal analysis carried out on the same samples does not reveal appreciable differences among the different samples. By way of example, Fig. 3 displays the thermogram of the apatite obtained after interaction with chloride in the range of pH 4 to 7, where it is possible to identify an endothermic broadened process up to about 950° C and an exothermic one, mostly due to sintering, at higher temperatures.

The optical microscopic analysis carried out on the tablets sintered at 1000° C reveals a shrinkage followed by a softening of the samples before melting. The ranges of temperature of shrinkage and the softening temperatures of the different products are reported in Table III. HA, F1 and F2 undergo, a constant shrinkage as a function of temperature, while the shrinkage of C11 and C12 increases with increasing temperature.

The grain sizes of the different apatitic products after sintering were determined by Hilliard's method [13, 14] from analysis of the scanning size D as a function of the time of firing in the range of temperature 900 to 1300° C is reported in Fig. 4.

TABLE II Weight losses of the apatitic products submitted to thermogravimetric analysis up to 1200° C.

Sample	Weight loss up to 900° C (%)	Weight loss up to 1200° C (%)	Total weight loss (%)
HA	2.8 ± 0.2	1.5 ± 0.1	4.3 ± 0.2
F1	0.5 ± 0.1	0.8 ± 0.1	1.3 ± 0.1
F2	3.5 ± 0.2	0.8 ± 0.1	4.3 ± 0.2
C11	0.5 ± 0.1	1.0 ± 0.1	1.5 ± 0.1
C12	3.5 ± 0.2	1.0 ± 0.1	4.5 ± 0.2

TABLE III Ranges of temperature of shrinkage and softening temperature of tablets sintered at 1000° C

Sample	Range of temperature of shrinkage (° C)	Softening temperature (° C)
HA	1000 to 1440	> 1460*
F1	1000 to 1410	> 1460*
F2	1000 to 1400	> 1460*
C11	1140 to 1450	1450
C12	1140 to 1450	1450

*1460° C represents the upper limit of temperature of our Leitz microscope.

4. Discussion and conclusions

The diffractometric and chemical analyses reveal that under cyclic pH fluctuation fluoride substitutes for hydroxyl ions in the apatite structure, in agreement with previous results [8]. On the other hand, the slight reduction of the lattice parameters observed in the samples C11 and C12 with respect to those of pure HA, must be attributed to the process of pH fluctuation. In fact, HA submitted to pH fluctuation in the absence of foreign ions exhibits cell parameters [8] very close to those calculated for C11 and C12. Therefore, under conditions of cyclic pH fluctuation chloride does not enter the crystal lattice of HA, as confirmed by the results of chemical analyses. However, the presence in solution of either fluoride or chloride prevents the incorporation of carbonate. In fact, the infrared absorption analysis reveals that F1 and C11 contain smaller amounts of carbonate with respect to HA, while the greater amount of carbonate incorporation observed in F2 and C12 is probably due to the high value of the upper limit of pH fluctuation. The position of the IR absorption bands of carbonate is in agreement with a substitution for phosphate groups (B-carbonate apatite) [5]. The different weight losses determined by thermogravimetric analysis are consistent with the different carbonate contents of the samples revealed by infrared absorption analysis.

Since carbonate ions are no longer present in the apatitic samples after heating at 1000° C (Fig. 3), the different behaviour of the sintered samples observed in the electron microscope as a function of temperature must be ascribed either to the effect of cyclic pH fluctuation or to the replacement of fluoride for hydroxyl in the apatite crystal structure.

No appreciable difference in the grain growth of the different apatitic products submitted to the sintering process has been determined. In fact, all the plots of log D (grain diameter) against log t (time) are straight lines with slopes falling between 0.25 and 0.40, so suggesting that a cubic grain growth (volumic) takes place [15].

In conclusion, the differences in carbonate and/or fluoride content of the samples examined do not appreciably affect the grain growth during sintering, while the method of synthesis seems to produce small differences in the technological behaviour of sintered samples.

Acknowledgements

The authors are grateful to the Italian National Researches Council and the Public Education Ministry of Italy, for financial support. They also wish to thank Mr M. Gandolfi for excellent technical assistance.

References

1. D. F. WILLIAMS, "Definitions in Biomaterials", Progress in Biomedical Engineering Vol. 4, European Society for Biomaterials (Elsevier, Amsterdam, 1987).
2. A. ENGSTROM, in "The Biochemistry and Physiology of Bone", edited by G. H. Bourne (Academic, London, 1972) pp. 237–258.
3. D. McCONNEL, "Applied Mineralogy", Vol 5 (Springer, Wein, 1973).
4. G. MONTEL, *Coll. Int. CNRS* **230** (1975) 13.
5. R. Z. Le GEROS, O. R. TRAUTZ, J. P. Le GEROS and E. KLEIN, *Science* **155** (1967) 1409.
6. R. A. YOUNG, *Coll. Int. CNRS* **230** (1975) 21.
7. R. Z. Le GEROS, L, M. SILVERSTONE, G. DACULSI and L. M. KEREBEL, *J. Dent. Res.* **62** (1983) 138.
8. A. BIGI, E. FORESTI, A. RIPAMONTI and N. ROVERI, *J. Inorg. Biochem.* **27** (1986) 31.
9. M. I. KAY, R. A. YOUNG and A. S. POSNER, *Nature* **204** (1964) 1050.
10. E. J. DUFF, *Chem. Ind.* (1974) 349.
11. E. J. DUFF and J. L. STUART, *Anal. Chim. Acta* **52** (1970) 155.
12. W. D. BISHOP and R. G. DHANESHWAR, *Anal. Chem.* **36** (1964) 726.
13. J. E. HILLIARD, Research Laboratory Report No. 62-RL-3133M (General Electric Co., Schenectady, New York, 1962).
14. *Idem, Metal Progr.* **85** (1964) 99.
15. W. D. KINGERY, H. K. BOWEN and D. R. UHLMANN, "Introduction to Ceramics", 2nd Edn (Wiley–Interscience, New York, 1976).

Received 29 July 1988
and accepted 3 May 1989